The Parasitic Capacitance of Magnetic Components with Ferrite Cores Due to Time-Varying Electromagnetic (EM) Field

Hui Zhao, Yiming Li, Qiang Lin and Shuo Wang

Power Electronics and Electrical Power Research Lab
Department of Electrical and Computer Engineering
University of Florida
Gainesville, FL 32611
zhaohui@ufl.edu

***Abstract*—The parasitic capacitance of a magnetic component, such as an inductor and a transformer, is critical because it can determine component's high frequency impedance, leading to voltage / current spikes, and causing EMI issue. The simulation-based techniques, the measurement-based techniques and the calculation-based techniques are popularly employed to model the parasitic capacitance. Measurement-based techniques are accurate in calculating the parasitic capacitance. The measurement-based techniques are black-box techniques and cannot provide guidelines in reducing the parasitic capacitance during manufacturing. The calculation-based techniques extract the parasitic capacitance based on calculated electric energy. Choosing the winding structure with reduced electric energy can also reduce the parasitic capacitance. However, when calculating the electric energy, the existing techniques are based on the quasi static approximation in which the electric field excited by the time-varying magnetic field is ignored. Simulation issues such as convergence issue exist in the simulation-based techniques. This paper focuses on the solution of comprehensive calculation of all the parasitic capacitance, including both the electrostatic capacitance and the time-varying EM capacitance. It proves that for the magnetic components with ferrite cores, the time-varying EM capacitance can be the dominant capacitance for high frequency magnetic components and it cannot be ignored. Therefore, it explained why the calculated capacitance is not accurate for certain type magnetic components. Furthermore, the paper proposes certain structures to achieve small parasitic capacitance.**

***Keywords*—Parasitic capacitance, electrostatic analysis, time varying electromagnetic (EM) field, high-frequency inductors/transformers**

I. INTRODUCTION

Magnetic components such as inductors / transformers are the basic components for electrical and electronic systems. In 1914, W. Lenz discovered that, at a certain frequency the impedance of an inductor would reach a resonance and then the impedance of the inductor become capacitive [1]. In 1915, J. L. Thompson and S. A. Stigant [2] defined the capacitance as the self-capacitance and pointed out this self-capacitance could lead to over-voltage because of resonance. [2] also pointed out that large parasites can cause voltage and current overshot. [3] pointed out high frequency impedance and electromagnetic interference (EMI) noise are dominated by the parasite parameters. Therefore, the parasites are critical especially for the high frequency domain. [2, 4, 5] proposed techniques to extract the parasitic parameters using impedance measurement, s-parameter measurement and time domain reflectometry method. Most research [6-8] focused on reducing the parasitic capacitance to achieve an inductive impedance for a high frequency range. Some research investigated on the utilization of the parasitic capacitance. For example, [9, 10] control the parasitic capacitance to form a balanced wheatstone bridge and to reduce the common EMI noise.

To model the parasitic capacitance, the measurement-based techniques and calculation-based techniques are widely applied. For typical measurement-based techniques, based on the measured impedance curve, [2] used equivalent parasitic capacitance (EPC) to model the parasitic capacitance, so that the impedance of the proposed model with parasitic capacitance can predict the measured impedance. Optimization tools [11] can be applied to determine the parameters of the EPC. However, the measurement-based techniques are essentially a black-box based techniques. The physical meaning of the EPC is vague, and it is unclear that how to design / reduce the parasitic capacitance. Therefore, the calculation-based techniques are necessary.

Recently, one of the most distinguished researches on parasitic capacitance calculation is leaded by J. W. Kolar's group [12, 13]. The papers discussed the physical meaning, calculation method, and rigorous equation of the parasitic capacitance of the inductors. The differences between calculation and measurement results are below 30%, which is

This research was supported by National Science Foundation under Award Number 1611048.

Authorized licensed use limited to: LAHORE UNIV OF MANAGEMENT SCIENCES. Downloaded on July 21,2020 at 18:00:07 UTC from IEEE Xplore. Restrictions apply.

very small. However, the calculated capacitance is always smaller than the measured capacitance, and this negative deviation indicates that some parasitic capacitance is not included in the proposed techniques. Moreover, group [12, 13] only concentrated on some specific applications, such as high voltage transformers. It is still unclear if the calculated capacitance is effective for all cases. Up to now, the most valuable technique for parasitic capacitance extraction for both research and industry is still the measurement-based techniques. Even in 2017, a measurement-based technique is still proposed [14] to extract the parasitic capacitance of the magnetic components.

For all the existing calculation-based techniques, the parasitic capacitance is to represent the energy of the electric field [12, 13, 15] and is based on the quasi static approximation to simplify the calculation procedure. However, the time-varying magnetic field can excite the time-varying electric field. If the time-varying electric field is dominated, the corresponding capacitance cannot be ignored.

Literatures usually include the capacitance extracted from the commercial software, such as Ansys Maxwell and Q3D, with finite-element method (FEM). However, both Maxwell and Q3D do not include the time-varying simulation when extracting the parasitic capacitance.

This paper derives the comprehensive expressions and considers both the quasi-static electric energy and time-varying EM electric energy. With the derived expression, it discovers that the electric field inside the ferrite core due to the time-varying (EM) field is significant. In some practical cases, if only electrostatic energy is considered as in the existing techniques, the corresponding capacitance could be neglected inappropriately. The paper derives the equation of the parasitic capacitance based on the electric energy inside the magnetic core. Then it discusses the conditions in which this capacitance cannot be ignored. Simulation and experiments have been conducted to verify the existence of this parasitic capacitance and the accuracy of the equation. It should be noted that the electrostatic simulation and time-varying EM simulation results are much different from each other, which indicates that the capacitance due to time-varying EM field should be considered.

The paper is organized as follows: in section II, the existent explanation of inductor parasitic capacitance based on electrostatic energy is briefly reviewed and the issue is pointed out; in section III, the parasitic capacitance due to time-varying EM field is derived and an improved parasitic model of an inductor is proposed; in section IV, the paper discusses about the practical conditions in which the parasitic capacitance inside the core is significant; in section V, simulation and experiment results verify the derivation and discussion.

II. The Existing Calculating-Based Techniques for Parasitic Capacitance and their Issues

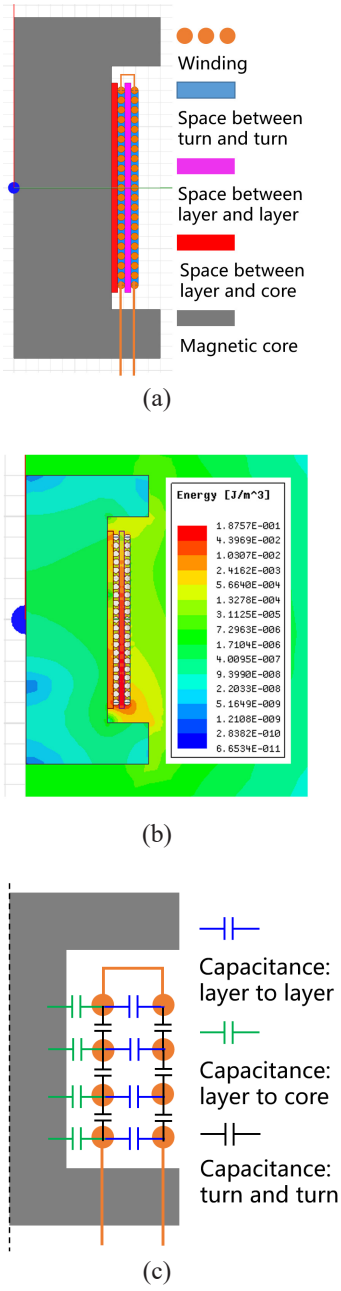

Fig. 1. The illustration of EPC in a rod inductor. (a) the spaces corresponding to each parasitic capacitance; (b) the simulated electrostatic energy in the spaces with Maxwell, and (c) parasitic capacitances in a rod inductor.

Parasitic capacitance is the component to represent the stored energy in an electric field and can be used to model the V-I curve (the impedance curve). The expression between the equivalent parasitic capacitance (EPC) and the stored energy with given voltage is:

Authorized licensed use limited to: LAHORE UNIV OF MANAGEMENT SCIENCES. Downloaded on July 21,2020 at 18:00:07 UTC from IEEE Xplore. Restrictions apply.

$$W_E = \frac{1}{2} C V^2 \quad (1)$$

From (1), the EPC can be derived as shown in (2):

$$EPC = 2\frac{W_E}{V^2} \quad (2)$$

Therefore, if the electric energy generated by an inductor is determined, its EPC can be derived. The existing techniques separates the parasitic capacitances of inductors / transformer into three portions: turn-to-turn capacitance, layer-to-layer capacitance and the winding-to-core capacitance [3]. Fig. 1 (a) shows these capacitances in a rod inductor. Each parasitic capacitance can be calculated separately via (1) and (2). And a basic inductor model with its EPC can thus be determined.

A. Conventional Techniques on Calculating Capacitance

Existing techniques focus on five portions of the parasitic capacitance: the turn-to-turn capacitance, the layer-to-layer capacitance, the winding-to-magnetic core capacitance, the winding to electrostatic screen capacitance and the interwinding capacitance. This section aims to analyze how conventional technique would calculate the parasitic capacitance based on the static-electric field and reduce the parasitic capacitance based on the analysis. Moreover, it also points out that even the conventional techniques realize that the static assumption is not accurate enough and how they further reduce calculation-error.

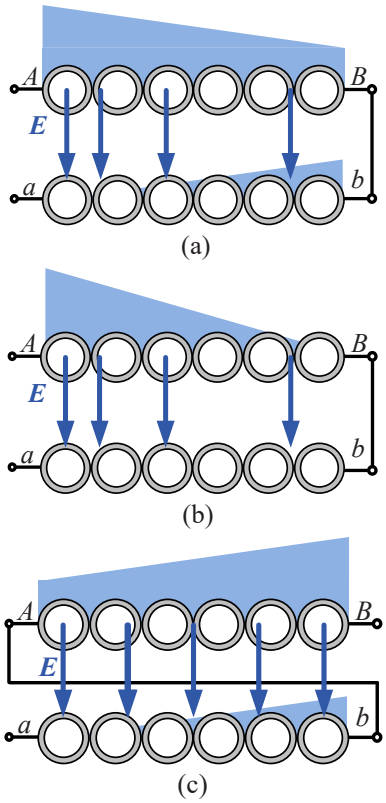

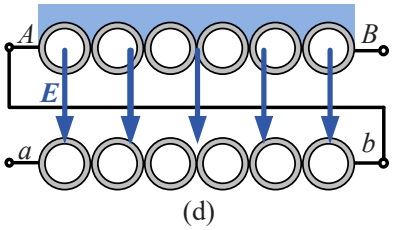

Fig. 2. The calculation and optimization of layer-to-layer capacitance: (a) the conventional connection where terminal *A* is connected to *b*; (b) the equivalent voltage potential distribution of the conventional connection; (c) the optimized connection: terminal *B* is connected to *b*; and (d) the equivalent voltage potential distribution of the optimized connection.

A simulation is conducted in Ansys Maxwell to show this conclusion. Fig. 1 (a) shows the configuration and Fig. 1 (b) shows the simulated electric energy in the space. Based on simulation result, most of the electric energy is stored in space between turn and turn, between layer and layer and between layer and the magnetic core. The energy inside the core and outside of the inductor can be ignored.

Fig. 2 shows a double-layer winding, where the upper layer's terminals are *A* and *B*; the lower layer's terminals are *a* and *b*. The blue region represents the voltage potential for each winding. In Fig. 2 (a), terminal *B* is connected to *b*. Assume terminal *a*'s voltage potential is zero and terminal *B*'s voltage potential is *V*. The voltage potential difference between the upper layer *AB* and the lower layer *ab* is shown in Fig. 2 (b) and it varies from *V* to 0 along the winding *ab*. If the terminal *A* is connected to *b*, as shown in Fig. 2(c), the voltage difference will be as shown in Fig. 2(d) and it's different from (b), which is a constant *0.5V*. If it's assumed that the voltage is evenly distributed along the windings and the parasitic capacitance is evenly distributed between two adjacent layers [10, 15], the energy stored between layers in the case shown in Fig. 2(a, b) and (c, d) can be obtained by integrating along the winding, as shown in (3) and (4), respectively.

$$E_{Ly-Ly-ab} = \frac{1}{6} C_{Ly\_Ly} V^2 \quad (3)$$

$$E_{Ly-Ly-cd} = \frac{1}{8} C_{Ly\_Ly} V^2 \quad (4)$$

where $C_{ly\text{-}ly}$ is the total capacitance between two layers.

When considering the two-layer winding as a plate capacitor, the value of $C_{ly\text{-}ly}$ is $\varepsilon_r \varepsilon_0 (2\pi r w / d)$, where w is the length of each section, r is the radius of the winding, and d is the distance between each layer.

From (3) and (4), changing the connection type can reduce the total electric energy. Therefore, the corresponding parasitic capacitance can also be reduced. Therefore, the calculation-based technique is useful in reduce/optimize the parasitic capacitance.

Authorized licensed use limited to: LAHORE UNIV OF MANAGEMENT SCIENCES. Downloaded on July 21,2020 at 18:00:07 UTC from IEEE Xplore. Restrictions apply.

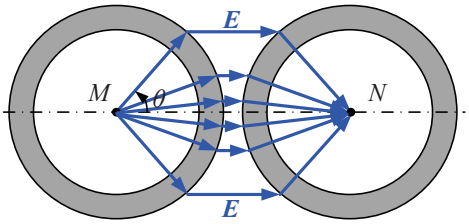

Fig. 3. Turn-turn capacitance calculation based on the assumption that the electric flux flows through the shortest path in the air-gap between two adjacent turns.

Another example is to calculate the turn-to-turn capacitance as shown in Fig. 3. An reasonable estimation is to assume that 1) the windings are infinit long, and 2) the charges along the wires are evenly distributed. Therefore, the capacitance between these two wires are as below:

$$C_t = \varepsilon_r \varepsilon_0 \frac{2\pi}{\ln(d_e / d_i)} \tag{5}$$

However, the second assumption does not hold for high frequency range. Massarini [16] assumed that the electric field between two wires follows the shorter path in the air-gap between the turns as shown in Fig. 3, and achieved a modified capacitance equation as shown below:

$$C_{t-t} = \varepsilon_r \theta^* \ln^{-1}\left(\frac{d_e}{d_i}\right) + \varepsilon_0 \cot\left(\frac{\theta^*}{2}\right) - \varepsilon_0 \cot\left(\frac{\pi}{12}\right) \tag{6}$$

where

$\theta^* = \arccos\left(1 - \frac{1}{\varepsilon_r} \ln\left(\frac{d_e}{d_i}\right)\right)$, ε_r is the relative permittivity of the outer insulation layer of the wire, d_e is the outer diameter of the wire, and d_i is the inner diameter of the wire.

The necessity of correcting turn-to-turn capacitance shows that the quasi-static assumption impacts the accuracy of the capacitance equation. However, [16] only considers the charging distribution caused by the time-varying EM. The electric field inside the core is still ignored.

B. Issues of the Existing Techniques

Although the existent model seems effective and can be verified with simulation, there's a phenomenon that cannot be explained by above theory. A setup in Fig. 4 (a) is shown to illustrate the phenomenon. In Fig. 4 (a), a one-turn inductor is formed by a wire passing through a ferrite toroid core and its impedance is measured as shown in Fig. 4 (b). The distance between the wire and the core is greatly increased and the area of the wire is decreased enough so that the capacitance between the wire and the core can be ignored. Based on the analysis of section II. A, the EPC of the inductor should be very small and can be ignored.

However, the measurement result shows that the inductor becomes capacitive at 2 MHz and the capacitance is still unneglectable. Moreover, when the relative position of the wire and the core is changed, the parasitic capacitance does not change, which indicates there's another parasitic capacitance need to be considered.

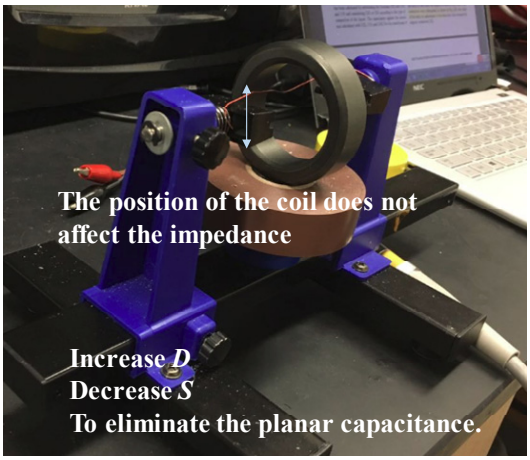

(a)

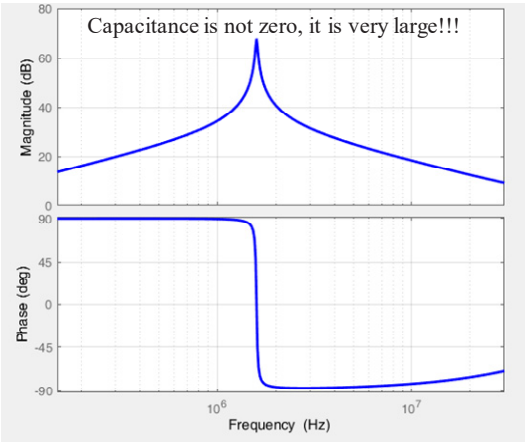

(b)

Fig. 4. (a) A setup used to change the distance between core and conductor; (b) Measured impedance of the inductor under test.

III. Time-Varying EM Field inside Magnetic Core and the Corresponding Capacitance

For convenience, a toroidal core is chosen as an example to derive the capacitance due to electromagnetic field inside the core as shown in Fig. 5 (a). The radius of the core is R_o and the radius of the cross-section area is R_i. Fig. 5 (b) shows the H field induced by the current flowing through the coil and Fig. 5 (c) shows the E field induced by the H field inside the core.

Based on Ampere's Law in (7), the H-field inside the core is obtained, where N is the turn number and I is the RMS value of current in the coil. The current flowing in the coil can be represented by $i(t) = \sqrt{2} I \cdot \sin(\omega t)$. The B-field inside the core can be obtained as shown in (8), where $l = 2\pi R_o$.

Authorized licensed use limited to: LAHORE UNIV OF MANAGEMENT SCIENCES. Downloaded on July 21,2020 at 18:00:07 UTC from IEEE Xplore. Restrictions apply.

$$\oint Hdl = NI \tag{7}$$

$$B = \frac{\mu NI}{l} \tag{8}$$

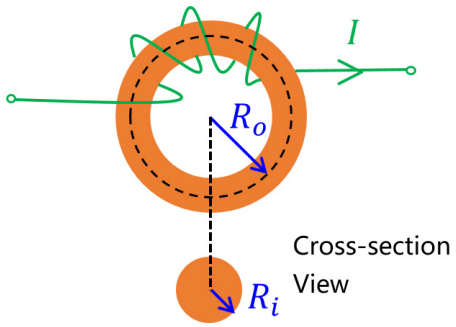

(a)

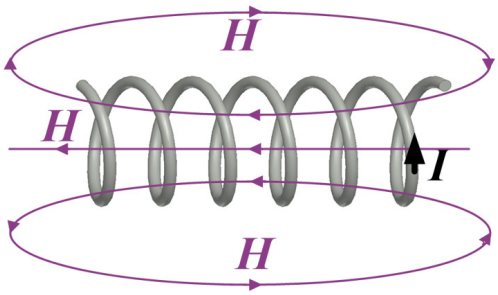

(b)

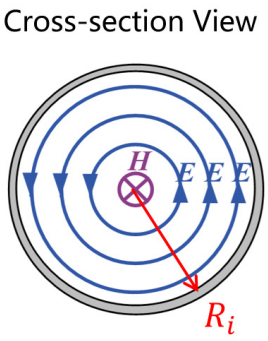

(c)

Fig. 5. (a) A toroidal core and its cross-section view; (b) H-field induced by current flowing through the coil and (c) E-field induced by H-field.

Based on Faraday's Law in (9), the E-field inside the core can also be obtained as shown in (10). In (10), the origin is at the center of the cross-section circle and r shows the distance to the origin.

$$\oint Edl = -\frac{\partial}{\partial t}\int_S BdS \tag{9}$$

$$E(r,t) = -\frac{\sqrt{2}}{2}\frac{\omega\mu NI}{l}\cdot r\cdot\cos(\omega t) \tag{10}$$

Therefore, the electric energy density can be represented with (11) and the total electric energy inside the core can be calculated as shown in (12).

$$w_E(r) = \frac{1}{2}\varepsilon\left(E(r)\right)^2 \tag{11}$$

$$W_E = \iiint_V w_E(r)dV = \frac{\pi}{16}\cdot\frac{\varepsilon\mu^2\omega^2N^2I^2R_i^4}{l} \tag{12}$$

Since the inductor's voltage can be obtained based on the geometry structure if the inductor current I is given, the equivalent parasitic capacitance inside the core, C_{Core}, can be solved using (2). (13) shows equation of inductor voltage, where V is the RMS value. (14) shows the equation of C_{Core}.

$$V = \mu\omega\pi\frac{N^2R_i^2}{l}\cdot I \tag{13}$$

$$C_{Core} = \frac{\varepsilon l}{8\pi N^2} \tag{14}$$

From (14), it's clear that the capacitance inside the core is determined by the turn number, magnetic path length and permittivity of the core. As turn number increases, this capacitance will greatly decrease.

Based on given conditions, the inductance of the inductor L can also be obtained, as shown in (15). If C_{Core} is much larger than other parasitic capacitances such as layer-layer capacitance, the resonance frequency f_R of the inductor is determined by L and C_{Core}, as shown in (16).

$$L = \mu\frac{N^2\pi R_i^2}{l} \tag{15}$$

$$f_R = \frac{1}{2\pi}\cdot\sqrt{\frac{1}{LC_{Core}}} = \frac{1}{\pi R_i}\cdot\sqrt{\frac{2}{\mu\varepsilon}} \tag{16}$$

An important conclusion can be drawn from (16). For a magnetic core, if C_{Core} dominates the EPC, the self-resonance is independent of turn number. It's only determined by its material and the cross-section area. It indicates for an inductor made with any material, it's impossible to extend the effective frequency range infinitely.

It should be pointed out that the time-varying EM field inside a core will generate not only capacitance, but also power loss. The power loss density inside the core due to time-varying EM field can be represented with (17), where σ is the conductance of the core. The total power loss can be calculated as shown in (18). Similarly, the equivalent resistance of the core, R_{Core}, can be derived as (19).

$$p(r) = \sigma\cdot\left(E(r)\right)^2 \tag{17}$$

Authorized licensed use limited to: LAHORE UNIV OF MANAGEMENT SCIENCES. Downloaded on July 21,2020 at 18:00:07 UTC from IEEE Xplore. Restrictions apply.

$$P = \iiint_V p(r)dV = \frac{\pi}{8} \cdot \frac{N^2 \mu^2 \sigma \omega^2 R_i^4}{l} \tag{18}$$

$$R_{Core} = \frac{V^2}{P} = \frac{8\pi N^2}{\sigma l} \tag{19}$$

Based on (14), C_{Core} is proportional to the permittivity of the magnetic core. For materials with relative small permittivity, such as iron powder cores, C_{Core} can be ignored when calculating the EPC of an inductor. However, for ferrite core with soft material [17] which is commonly used in industry, both the permittivity and permeability is high. The electric field within the core is high. Therefore, without considering the electric field within the core, the calculated capacitance will be smaller than the measured capacitance. Also, since the turn number will also influence C_{Core}, for an inductor with a large turn number or even multi-layer winding, the EPC could be very large and C_{Core} can also be ignored.

Ferrite cores are usually applied for the high frequency common mode (CM) inductors/chokes in AC/DC adapters since the inductance can be significant with just a few turns. However, at high frequency, the CM inductor will become capacitive to the detriment of its EMI performance. Since the high frequency CM choke usually applies single layer winding structure in order to reduce its EPC, the case discussed in section III fits for this application. Based on (16), if the cross-section area can be designed smaller, the resonance frequency will increase, which helps to improve its high frequency performance.

IV. Simulations and Experiments

A ferrite toroid core with high permittivity (N84) is applied to verify the theory in this paper. The permittivity is measured with Keysight impedance analyzer E4990A. Three techniques proposed in Keysight's Application Note [18], and their comparison is as shown in Table I. To achieve the highest accuracy with simple operation, the contacting electrode with thin film electrode is proposed in this paper.

Contacting electrode method is as shown in Fig. 6. This method derives permittivity by measuring the capacitance of the electrodes contacting the material under test (MUT) directly as show in Fig. 6 (a). Permittivity and loss tangent are calculated using the equations below:

$$\begin{cases} Y = \dfrac{1}{Z} = G + j\omega C_p \\ \varepsilon_r = \dfrac{t_m C_p}{A\varepsilon_0} \end{cases} \tag{20}$$

where Z is the impedance measured from the impedance analyzer, Y is the admittance calculated from Z, G is the real part of Y, ω is the frequency, C_p is equivalent parallel capacitance of MUT [F], t_m is average thickness of MUT [m], A is guarded electrode's surface area [m^2], ε_0 is absolute permittivity which equals 8.854e-12 [F/m].

The contacting electrode method requires no material preparation and the operation involved when measuring is simple. Therefore, it is the most widely used method. However, a significant measurement error can occur if airgap and its effects are not considered when using this method. When contacting the MUT directly with the electrodes, an airgap is formed between the MUT and the electrodes. No matter how flat and parallel both sides of the MUT are fabricated, an airgap will still form. In this paper, instead of using the fixture of Keysight, this airgap effect can be eliminated by making electrodes applying conductive adhesive to the surfaces of the dielectric material. The most accurate measurements can be performed. The measurement result is as shown in Fig. 7 with the given N84 material.

Table I. Comparison of parallel plate measurement methods

Method	Contacting electrode	Non-contacting electrode	Contacting electrode (with thin film electrode)
Accuracy	LOW	MEDIUM	HIGH
Operation	1 measurement	2 measurements	1 measurement

A time-varying EM field simulation is done in Ansys HFSS environment. Unlike Maxwell or Q3D, HFSS does not have the assumption that the system is in a quasi-static field. It is a common belief that the results from Maxwell, Q3D and HFSS matches with each other within a low frequency range. The configuration of the inductor is shown in Fig. 8 (b) and the E-field is shown in Fig. 8 (c). Based on the simulation, the distribution of electric field inside the core is also identical to the analysis in section III. It should be noted that in an electrostatic field simulation (as shown in Fig. 1(c)), there's no such an E-field inside the core.

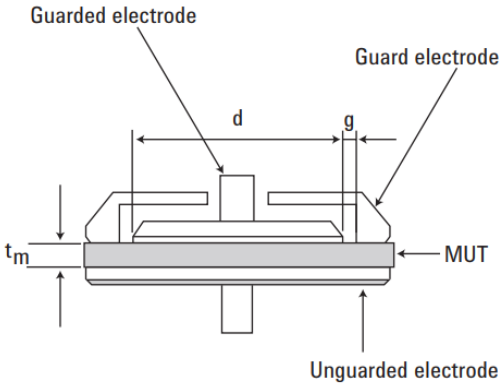

(a)

Authorized licensed use limited to: LAHORE UNIV OF MANAGEMENT SCIENCES. Downloaded on July 21,2020 at 18:00:07 UTC from IEEE Xplore. Restrictions apply.

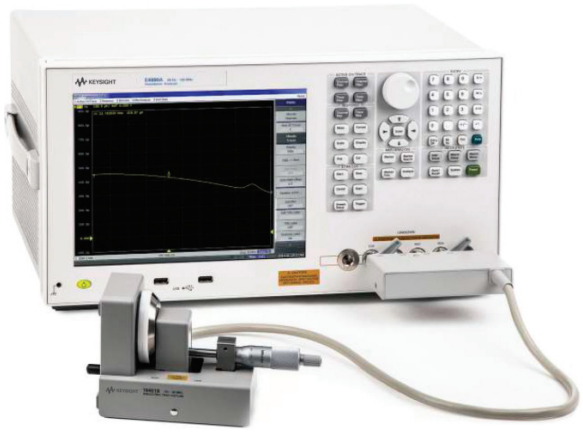

(b)

Fig. 6. (a) the diagram of the contacting electrode method; and (b) the photo showing the permittivity measurement.

The turn number is changed from 1 to 3 and the impedance of the inductor is measured. Based on the measurement result shown in Fig. 8 (a), as the turn number increases, the resonance frequency where the inductor becomes capacitive is constant, which is identical to (16).

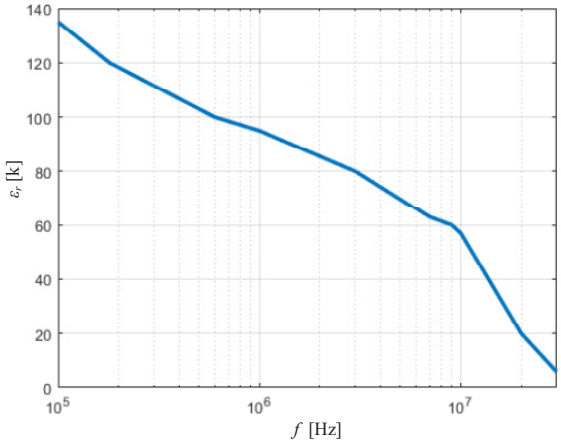

Fig. 7. The measured permittivity of N84 material within [150e3, 30e6]Hz.

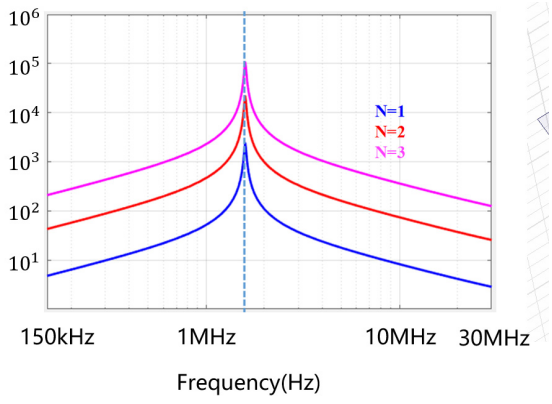

(a)

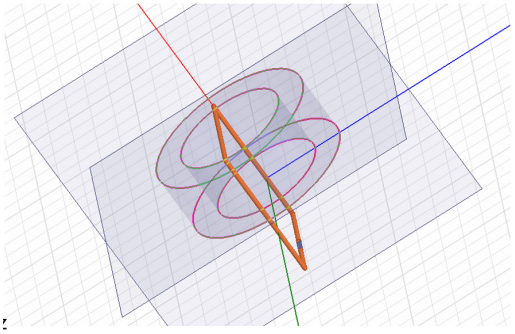

(b)

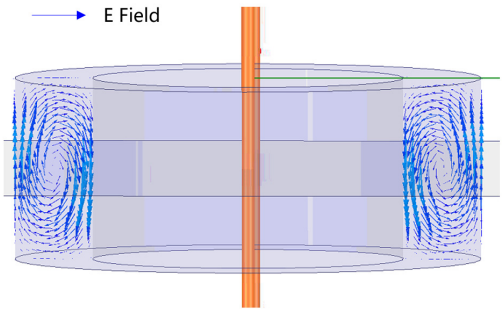

(c)

Fig. 8. (a) Impedance measurement results of a ferrite toroid inductor with very few turns; (b) Configuration of toroid core applied in time-varying EM field simulation and (c) E-field distribution inside the core form HFSS simulation.

V. Conclusion

This paper derived the equation of the parasitic capacitance due to the time-varying electromagnetic field inside the magnetic core. It explained the inaccuracy of the current equations and constant self-resonance frequency phenomena and predicted the frequency limitation of an inductor. Based on this derived equation, this capacitance can be dominated in the inductors with small turn number or single winding layer, which is practical in high frequency common mode choke design. Simulations and experiments verified the phenomena and explanation.

In the future, more experiments and simulations need to be done to verify the results. Also, based on the derived equation, an analysis on modifying the inductor structure to reduce the parasitic capacitance inside the core and improve the high frequency performance need to be investigated. More applications can be developed based on the discovery.

Authorized licensed use limited to: LAHORE UNIV OF MANAGEMENT SCIENCES. Downloaded on July 21,2020 at 18:00:07 UTC from IEEE Xplore. Restrictions apply.

REFERENCES

[1] W. Lenz, "Calculation of the free period of a single layer coill," *Annal. Phys,* vol. 43, pp. 49-97, 1914.

[2] J. L. Thompson and S. A. Stigant, "Overvoltages in transformers due to the self-capacity of the windings," *Elect. Rev.,* vol. 76, pp. 25-37, 1915.

[3] S. Wang, F. C. Lee, D. Y. Chen, and W. G. Odendaal, "Effects of parasitic parameters on EMI filter performance," *Power Electronics, IEEE Transactions on,* vol. 19, no. 3, pp. 869-877, 2004.

[4] S. Wang, F. C. Lee, and W. G. Odendaal, "Characterization and parasitic extraction of EMI filters using scattering parameters," *Power Electronics, IEEE Transactions on,* vol. 20, no. 2, pp. 502-510, 2005.

[5] Z. Huibin, A. R. Hefner, and L. Jih-Sheng, "Characterization of power electronics system interconnect parasitics using time domain reflectometry," *Power Electronics, IEEE Transactions on,* vol. 14, no. 4, pp. 622-628, 1999.

[6] J. L. Kotny, X. Margueron, and N. Idir, "High-Frequency Model of the Coupled Inductors Used in EMI Filters," *IEEE Transactions on Power Electronics,* vol. 27, no. 6, pp. 2805-2812, 2012.

[7] W. Zhang, Y. Su, M. Mu, D. J. Gilham, Q. Li, and F. C. Lee, "High-Density Integration of High-Frequency High-Current Point-of-Load (POL) Modules With Planar Inductors," *IEEE Transactions on Power Electronics,* vol. 30, no. 3, pp. 1421-1431, 2015.

[8] W. Liang, L. Raymond, and J. Rivas, "3-D-Printed Air-Core Inductors for High-Frequency Power Converters," *IEEE Transactions on Power Electronics,* vol. 31, no. 1, pp. 52-64, 2016.

[9] S. Wang, P. Kong, and F. C. Lee, "Common Mode Noise Reduction for Boost Converters Using General Balance Technique," *Power Electronics, IEEE Transactions on,* vol. 22, no. 4, pp. 1410-1416, 2007.

[10] H. Zhang, S. Wang, Y. Li, Q. Wang, and D. Fu, "Two-Capacitor Transformer Winding Capacitance Models for Common-Mode EMI Noise Analysis in Isolated DC/DC Converters," *Power Electronics, IEEE Transactions on,* vol. 32, no. 11, pp. 8458-8469, 2017.

[11] H. Zhao, S. Wang, J. Min, and Y. Zhi, "Systematic modeling for a three phase inverter with motor and long cable using optimization method," in *2016 IEEE Energy Conversion Congress and Exposition (ECCE)*, 2016, pp. 1-8.

[12] L. Dalessandro, F. d. S. Cavalcante, and J. W. Kolar, "Self-Capacitance of High-Voltage Transformers," *IEEE Transactions on Power Electronics,* vol. 22, no. 5, pp. 2081-2092, 2007.

[13] F. d. S. Cavalcante and J. W. Kolar, "Small-Signal Model of a 5kW High-Output Voltage Capacitive-Loaded Series-Parallel Resonant DC-DC Converter," in *2005 IEEE 36th Power Electronics Specialists Conference*, 2005, pp. 1271-1277.

[14] C. Liu, L. Qi, X. Cui, and X. Wei, "Experimental Extraction of Parasitic Capacitances for High-Frequency Transformers," *IEEE Transactions on Power Electronics,* vol. 32, no. 6, pp. 4157-4167, 2017.

[15] E. Laveuve, J. P. Keradec, and M. Bensoam, "Electrostatic of wound components: analytical results, simulation and experimental validation of the parasitic capacitance," in *Conference Record of the 1991 IEEE Industry Applications Society Annual Meeting*, 1991, pp. 1469-1475 vol.2.

[16] A. Massarini and M. K. Kazimierczuk, "Self-capacitance of inductors," *IEEE Transactions on Power Electronics,* vol. 12, no. 4, pp. 671-676, 1997.

[17] Ferroxcube, "Application Note - Soft ferrite material survey," 2008.

[18] Keysight, "Application Note - Solutions for Measuring Permittivity and Permeability with LCR Meters and Impedance Analyzers," 2016.

[19] S. Wang, F. C. Lee and W. G. Odendaal, "Single layer iron powder core inductor model and its effect on boost PFC EMI noise," *Power Electronics Specialist Conference, 2003. PESC '03. 2003 IEEE 34th Annual*, 2003, pp. 847-852 vol.2.

[20] S. Wang, F. C. Lee and J. D. van Wyk, "Design of Inductor Winding Capacitance Cancellation for EMI Suppression," in *IEEE Transactions on Power Electronics*, vol. 21, no. 6, pp. 1825-1832, Nov. 2006.

[21] S. Wang, F. C. Lee and J. D. van Wyk, "Inductor winding capacitance cancellation using mutual capacitance concept for noise reduction application," in *IEEE Transactions on Electromagnetic Compatibility*, vol. 48, no. 2, pp. 311-318, May 2006.

[22] S. Wang and F. C. Lee, "Common-Mode Noise Reduction for Power Factor Correction Circuit With Parasitic Capacitance Cancellation," in *IEEE Transactions on Electromagnetic Compatibility*, vol. 49, no. 3, pp. 537-542, Aug. 2007.

[23] S. Wang and F. C. Lee, "Analysis and Applications of Parasitic Capacitance Cancellation Techniques for EMI Suppression," in *IEEE Transactions on Industrial Electronics*, vol. 57, no. 9, pp. 3109-3117, Sept. 2010.

[24] S. Wang and F. C. Lee, "Negative Capacitance and its Applications on Parasitic Cancellation for EMI Noise Suppression," *2007 IEEE Power Electronics Specialists Conference*, Orlando, FL, 2007, pp. 2887-2891.

Authorized licensed use limited to: LAHORE UNIV OF MANAGEMENT SCIENCES. Downloaded on July 21,2020 at 18:00:07 UTC from IEEE Xplore. Restrictions apply.